

Clogging and Transport of Driven Particles in Asymmetric Funnel Arrays

C. J. O. Reichhardt^{1, a)} and C. Reichhardt¹

Theoretical Division and Center for Nonlinear Studies, Los Alamos National Laboratory, Los Alamos, New Mexico 87545, USA

We numerically examine the flow and clogging of particles driven through asymmetric funnel arrays when the commensurability ratio of the number of particles per plaquette is varied. The particle-particle interactions are modeled with a soft repulsive potential that could represent vortex flow in type-II superconductors or driven charged colloids. The velocity-force curves for driving in the easy flow direction of the funnels exhibit a single depinning threshold; however, for driving in the hard flow direction, we find that there can be both negative mobility where the velocity decreases with increasing driving force as well as a reentrant pinning effect in which the particles flow at low drives but become pinned at intermediate drives. This reentrant pinning is associated with a transition from smooth one-dimensional flow at low drives to a clogged state at higher drives that occurs when the particles cluster in a small number of plaquettes and block the flow. When the drive is further increased, particle rearrangements occur that cause the clog to break apart. We map out the regimes in which the pinned, flowing, and clogged states appear as a function of plaquette filling and drive. The clogged states remain robust at finite temperatures but develop intermittent bursts of flow in which a clog temporarily breaks apart but quickly reforms.

A wide variety of both hard and soft matter systems can be modeled as particles that exhibit depinning phenomena under an external drive¹. Specific examples include vortices in type-II superconductors²⁻⁴, sliding charge density waves⁵, the depinning of electron crystals^{6,7} or colloidal assemblies⁸⁻¹⁰, and skyrmions in chiral magnets^{11,12}. In such systems, the depinning and subsequent sliding dynamics can be characterized using features in the velocity-force ($v - F$) curves. The particle velocity is zero in the pinned phase and becomes finite at a critical drive F_c . Within the moving phase the velocity can increase linearly with the driving force or it can show a series of steps corresponding to different effective depinning thresholds¹. It is also possible to observe negative differential mobility in which the velocity drops with increasing driving force due to changes in the flow pattern or the onset of different modes of dissipation^{1,13-16}. In some cases, the particles move in the direction opposite to the applied drive, producing absolute negative mobility^{17,18}. Many studies involve particles moving over an effectively two-dimensional (2D) substrate; however, depinning phenomena and nonlinear transport can also arise for particle flow in confined geometries such as quasi-one dimensional (1D) channels, constrictions¹⁹⁻²³, bottlenecks²⁴⁻²⁷, or asymmetric funnel arrays²⁸⁻³³. Pinning in these systems is produced by a confining effect of the walls, and particles that get stuck along the walls can reduce or stop the flow of other particles due to the particle-particle interactions. This pinning mechanism generates strong commensuration effects in which the critical drive F_c is enhanced when the number of particles is an integer multiple of the number of plaquettes or of any other periodicity in the system. Confined flow also appears in the motion of particulate matter through confining regions such as hoppers and bottlenecks, where clogging effects occur due to

steric particle-particle interactions³⁴⁻⁴¹. Similar effects arise in the flow of pedestrians or active matter through constrictions⁴²⁻⁴⁴.

In this work we consider an assembly of particles driven through a linear array of asymmetric funnels. The soft repulsive interactions between particles are modeled as a Bessel function $K_1(r)$ which decays exponentially at large r . This specific interaction potential describes vortices in type-II superconductors; however, a variety of simulation studies have shown that many of the behaviors observed for vortices interacting with pinning landscapes are generic to other systems of particles with similar interactions, such as charge-stabilized colloids with Yukawa interactions or magnetic colloids with dipolar interactions^{1,4,7,14,45,46}. Previous work on particles driven through funnel arrays focused on motion in the easy flow direction where the depinning force is low, and showed that a clear commensurability effect occurs whenever the number of particles is an integer multiple of the number of funnel plaquettes, while there is an overall increase in the depinning force with increasing commensurability ratio since crowding effects make it more difficult to force particles through the funnels³⁰. Here we consider particles driven in the hard direction of the funnel asymmetry. We find distinctive $v - F$ relations, include a clogging effect associated with reentrant pinning for increasing drive. In most systems that exhibit depinning phenomena, the velocity increases with increasing drive; however, we find that there are extended regions of drive and filling ratios in which reentrant pinning occurs. An initial depinning occurs at a low driving threshold F_{c1} when the particle density is uniform throughout the system, but at higher drives clogging events occur in which particles pile up in one or more of the funnels and block the flow, so that the velocity drops back to zero. As the drive increases further, particles can eventually force their way through the clog and allow the system to flow again above a second depinning threshold F_{c2} .

We argue that our results are consistent with clog-

^{a)}Corresponding author email: cjrx@lanl.gov

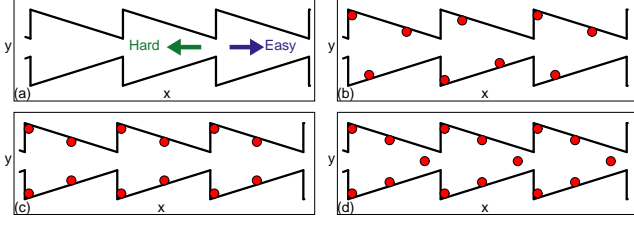


FIG. 1. (a) Illustration of a portion of the system showing the asymmetric funnel walls. In the initial state, each funnel plaquette holds N_c particles. A drive F_D is applied in the easy (right blue arrow) or hard (left green arrow) direction along the x axis. The full sample contains $N_{pl} = 16$ funnel plaquettes. (b,c,d) Illustrations of representative $F_D = 0$ particle configurations at $N_c =$ (b) 3.0, (c) 4.0, and (d) 5.0.

ging rather than jamming behavior. In a jammed state, particle-particle interactions cause the system to behave like a uniform rigid solid above a unique jamming density⁴⁷. In our system, although the initially pinned state and the flowing states are generally uniform, the reentrant pinned state is heterogeneous with local regions of high particle density. The reentrant pinning can occur for a wide range of fillings, as has been observed for clogging transitions⁴⁸, rather than only at a specific filling, as in the jamming transition. We discuss how our results could be relevant to vortices in superconductors, colloids in constriction geometries, Wigner crystals, and skyrmion systems, as well as how the behavior we observe is different from that found for particles with hard disk interactions such as grains or bubbles.

Simulation – We model a two-dimensional system with periodic boundaries in the x direction containing walls that form an asymmetric funnel array, as illustrated in Fig. 1. There are a total of $N_{pl} = 16$ funnel plaquettes, each of which initially contains N_c particles so that the total number of particles is $N_p = N_c N_{pl}$. The dynamics of particle i is governed by the following overdamped equation of motion:

$$\eta \frac{d\mathbf{R}_i}{dt} = - \sum_{j \neq i}^{N_p} \nabla U_{cc}(R_{ij}) - \mathbf{F}_{\text{wall}}^i + \mathbf{F}_D + \mathbf{F}_i^T. \quad (1)$$

We set the damping constant $\eta = 1.0$. The particle-particle interactions are repulsive and have the form $U_{cc}(R_{ij}) = A_0 K_0(R_{ij}/\lambda)$, where $R_{ij} = |\mathbf{R}_i - \mathbf{R}_j|$, $\mathbf{R}_{i(j)}$ is the position of particle $i(j)$, and K_0 is a Bessel function. We take λ to be the unit of distance in our simulation. The particle-particle interaction force is given by K_1 , which decays exponentially for $R_{ij} > \lambda$, allowing us to cut off the interactions for $R_{ij} > 6\lambda$. The unit of force in our simulation is A_0 . This model was previously used to study static vortex configurations in a funnel geometry as well as depinning and dynamics for driving in the easy flow direction³⁰.

The confining walls of each funnel plaquette are composed of 4 repulsive elongated potential barriers so

that the entire system contains $N_b = 4N_{pl}$ barriers. Each barrier consists of a rectangular repulsive region with a half-parabolic repulsive cap on each end. Particle-barrier interactions are described by $\mathbf{F}_{\text{wall}}^i = (f_p/r_p) \sum_{k=1}^{N_b} [R_{ik}^\pm \Theta(r_p - R_{ik}^\pm) \Theta(R_{ik}^\parallel - l_k) \hat{\mathbf{R}}_{ik}^\pm + R_{ik}^\pm \Theta(r_p - R_{ik}^\pm) \Theta(l_k - R_{ik}^\parallel) \hat{\mathbf{R}}_{ik}^\pm]$, where $f_p = 15A_0$, $R_{ik}^\pm = |\mathbf{R}_i - \mathbf{R}_k^\pm| \pm l_k \hat{\mathbf{p}}_{\parallel}^k$, $R_{ik}^{\pm, \parallel} = |(\mathbf{R}_i - \mathbf{R}_k^\pm) \cdot \hat{\mathbf{p}}_{\parallel}^k|$, \mathbf{R}_k^\pm is the position of the center point of barrier k , and $\hat{\mathbf{p}}_{\parallel}^k$ and $\hat{\mathbf{p}}_{\perp}^k$ are unit vectors parallel and perpendicular, respectively, to the axis of barrier k . The central rectangular barrier is of size $2l_k = 2.8\lambda$ for the vertical walls and $2l_k = 18\lambda/\sqrt{3}$ for the slanted walls. The barriers are arranged to form mirror-symmetric sawtooth shapes that produce the funnel array illustrated in Fig. 1(a).

Initially N_c particles are placed inside each funnel plaquette and allowed to thermally relax under simulated annealing using Langevin kicks \mathbf{F}^T that obey $\langle \mathbf{F}_i^T(t) \rangle = 0$ and $\langle \mathbf{F}_i^T(t) \mathbf{F}_j^T(t') \rangle = 2\eta k_B T \delta_{ij} \delta(t - t')$, where k_B is the Boltzmann constant. Once the temperature has been reduced to zero, we apply a driving force $\mathbf{F}_D = CF_D \hat{\mathbf{x}}$ with $C = +1$ for easy direction driving and $C = -1$ for hard direction driving. For each value of F_D we measure the average particle velocity $\langle V \rangle = N_p^{-1} \sum_i^{N_p} \mathbf{v}_i \cdot \hat{\mathbf{x}}$. We first consider driving in the absence of thermal fluctuations, but later we discuss the effect of finite temperature on the clogging dynamics.

Results – Illustrations of representative $F_D = 0$ particle configurations obtained through the annealing procedure appear in Fig. 1(b,c,d) for $N_c = 3.0, 4.0$, and 5.0 , respectively. At integer values of N_c , each plaquette captures N_c particles, while for noninteger values such as $N_c = 5.5$, there is a mixture of plaquettes containing 5 or 6 particles. A more complete study of the particle ordering at the zero drive condition is provided in Ref.³⁰. When a drive is applied in the positive x or easy flow direction, as in Ref.³⁰, the depinning force depends strongly on the commensuration ratio, as shown in Fig. 2(a). We plot four representative $\langle V \rangle$ versus F_D curves in Fig. 2(b) for driving in the easy flow direction at $N_c = 3.0, 4.0, 4.5$, and 5.0 . In each case, there is a single depinning threshold and $\langle V \rangle$ increases monotonically with increasing F_D . Other fillings produce similar $v - F$ curves.

In Fig. 3 we plot $|\langle V \rangle|$ versus F_D for driving in the negative x or hard direction for $N_c = 3.0, 3.25, 3.5$, and 3.75 . Here there are a variety of distinct dynamic behaviors and $v - F$ curve characteristics that are very different from those found for driving in the easy direction. For the commensurate filling of $N_c = 3.0$, there is a single depinning transition at $F_c = 0.02$ followed by a linear increase in $|\langle V \rangle|$ with increasing F_D . In Fig. 4(a) we show the particle trajectories for $N_c = 3.0$ at $F_D = 0.11$ where two particles are trapped at the corners of each plaquette and the remaining third of the particles move in a 1D channel along the negative x -direction.

In Fig. 3 at $N_c = 3.75$, there is still a single depinning threshold at $F_c = 0.0275$; however, a drop in $|\langle V \rangle|$ occurs near $F_D = 0.9$ indicating negative differential mo-

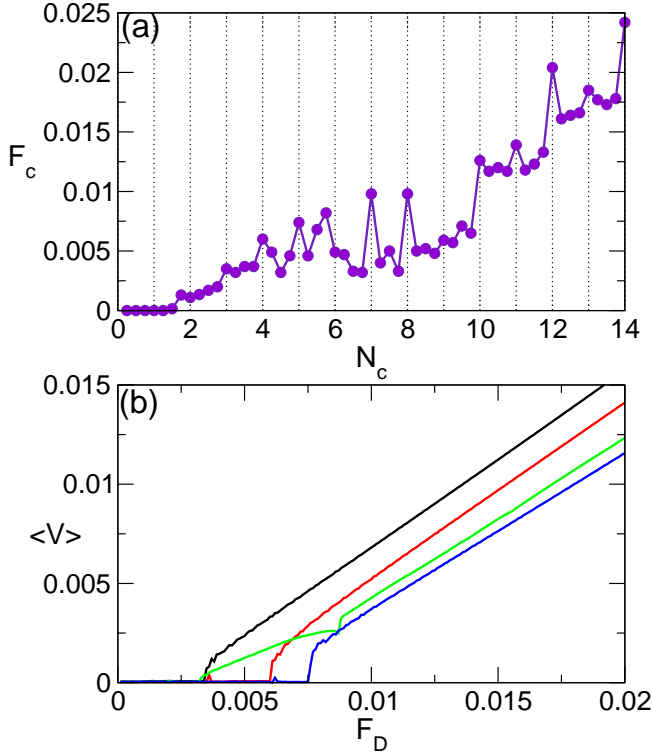


FIG. 2. (a) The depinning force F_c vs filling fraction N_c for driving in the easy direction with $C = +1$. (b) Representative $\langle V \rangle$ vs F_D curves for driving in the easy direction at $N_c = 3.0$ (black), 4.0 (red), 4.5 (green) and 5.0 (blue). In each case there is a single depinning threshold F_c .

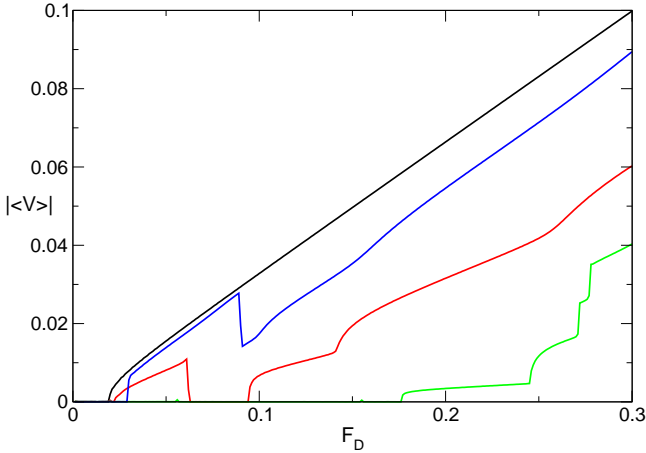


FIG. 3. The average particle velocity $|\langle V \rangle|$ vs F_D for driving in the hard direction with $C = -1$ for $N_c = 3.0$ (black), 3.25 (red), 3.5 (green), and 3.75 (blue). There is a single depinning transition for $N_c = 3.0$ and a region of reentrant pinning where $|\langle V \rangle|$ drops back to zero for $N_c = 3.25$. An example of negative differential conductivity appears for $N_c = 3.75$ in the form of a drop in $|\langle V \rangle|$ to a finite value near $F_D = 0.09$.

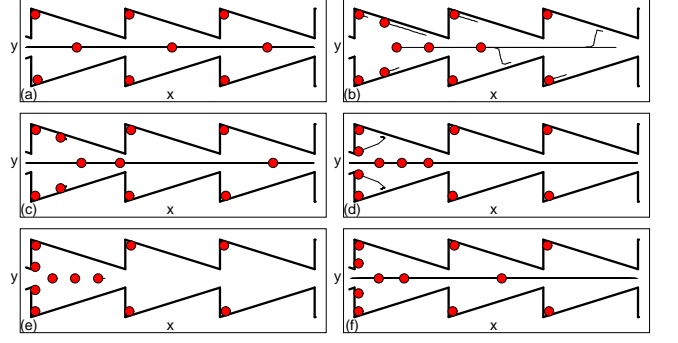


FIG. 4. The particle locations (circles) and trajectories (lines) for driving in the hard direction for the system in Fig. 3. (a) $N_c = 3.0$ at $F_D = 0.11$. (b-e) $N_c = 3.25$ for different F_D . (b) $F_D = F_{c1} = 0.022$. (b) The first sliding phase at $F_D = 0.044$. (c) The onset of the reentrant pinned phase at $F_D = F_{rp} = 0.0625$. (d) The reentrant pinned or clogged phase at $F_D = 0.088$, where there is an accumulation of particles in one of the plaquettes that blocks the flow of the other particles. (e) The sliding state at $F_D = 0.11$ above F_{c2} where the particles can move through the clog.

bility with $d\langle V \rangle / dF_D < 0$. For $N_c = 3.25$ we find a multi-step depinning process with an initial depinning at $F_{c1} = 0.022$. Above F_{c1} , $|\langle V \rangle|$ increases with increasing F_D until a drop to $|\langle V \rangle| = 0$ occurs over the interval of $0.0625 < F_D < 0.094$. This reentrant pinned phase is followed by a second depinning transition at $F_{c2} = 0.094$. In Fig. 4(b) we show the particle positions and trajectories just at F_{c1} , while Fig. 4(c) illustrates the particle flow in the first flowing region at $F_D = 0.044$. The transition into the reentrant pinned state appears in Fig. 4(d) for $F_D = 0.0625$. The reentrant pinning is triggered when two of the trapped particles in the plaquette shift their positions from sitting next to a slanted wall of the funnel to sitting next to a vertical wall of the funnel close to the leftmost funnel opening, as shown in Fig. 4(d). The shifted particles create a stronger repulsive barrier for the passage of other particles through the constriction on the left end of the funnel plaquette, causing the previously moving particles to be blocked, as plotted in Fig. 4(e) for the reentrant pinned phase at $F_D = 0.088$. The clog is characterized by the accumulation of an excess number of particles in a single plaquette. In this case, a similar clogging configuration appears in roughly every fourth plaquette, so the reentrant pinning can be viewed as a clogging event dominated by a small number of plaquettes. As F_D is further increased, there is a second depinning transition at F_{c2} to the second moving state illustrated in Fig. 4(f) at $F_D = 0.11$. Additional upward jumps in $|\langle V \rangle|$ can occur at higher F_D when additional particles in the clogged region become dislodged and join the flow.

A clogging phenomenon is also associated with the jump down in $|\langle V \rangle|$ versus F_D for $N_c = 3.75$, but in this case the clogging is only partial. In Fig. 5(a) we plot the 1D channel flow pattern in this system at $F_D = 0.066$

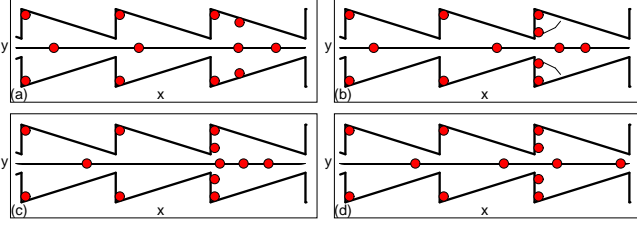


FIG. 5. The particle locations (circles) and trajectories (lines) for driving in the hard direction for the system in Fig. 3 at $N_c = 3.75$ where there is a region of negative differential conductivity. (a) The flowing phase at $F_D = 0.066$. (b) The shift in particle positions from the slanted walls to the funnel aperture at the drop in $|\langle V \rangle|$ at $F_D = 0.09$. (c) At $F_D = 0.12$, above the drop in $|\langle V \rangle|$, a partial clog forms when the particles next to the funnel aperture slow down the flow. (d) At $F_D = 0.26$, the size of the partial clog decreases.

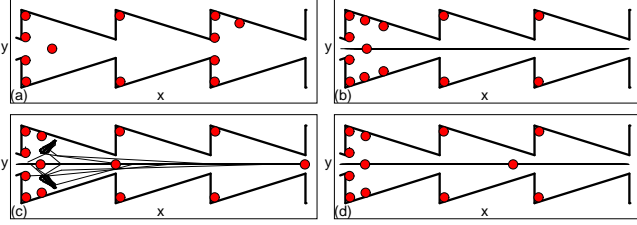


FIG. 6. The particle locations (circles) and trajectories (lines) for driving in the hard direction for the system in Fig. 3 at $N_c = 3.5$. (a) At $F_D = 0.15$, the system is in a clogged state with a buildup of particles in the leftmost plaquette. (b) The flow along the first velocity step at $F_D = 0.2$. (c) Multiple rearrangements of the particles occur at the second step in $|\langle V \rangle|$ centered at $F_D = 0.26$. (d) The flow above the second step in $|\langle V \rangle|$ at $F_D = 0.3$ where the partial clog is smaller.

prior to the drop in $|\langle V \rangle|$. As F_D increases, some trapped particles suddenly shift from sitting along the slanted walls to sitting next to the funnel aperture, as shown in the rightmost plaquette of Fig. 5(b) at $F_D = 0.09$. These particles constrict but do not stop the channel flow, resulting in a local accumulation of particles at the constriction, as illustrated in Fig. 5(c) at $F_D = 0.012$. As F_D is further increased, the flow gradually increases and the size of the partial clog reduces, as shown in Fig. 5(d) at $F_D = 0.26$.

For $N_c = 3.5$, the reentrant pinning is lost and F_{c1} increases to $F_{c1} = 0.175$ while the depinning occurs in a series of steps. The initial flow phase disappears due to the development of an instability within the pinned phase that causes particles to shift from the slanted walls to positions near the funnel aperture prior to the onset of 1D channel flow, producing a direct transition from the pinned state to a clogged state without an intermediate flowing phase. In Fig. 6(a) at $F_D = 0.15$, the system is already in a clogged state even though no steady state particle flow has occurred. The number of particles in each

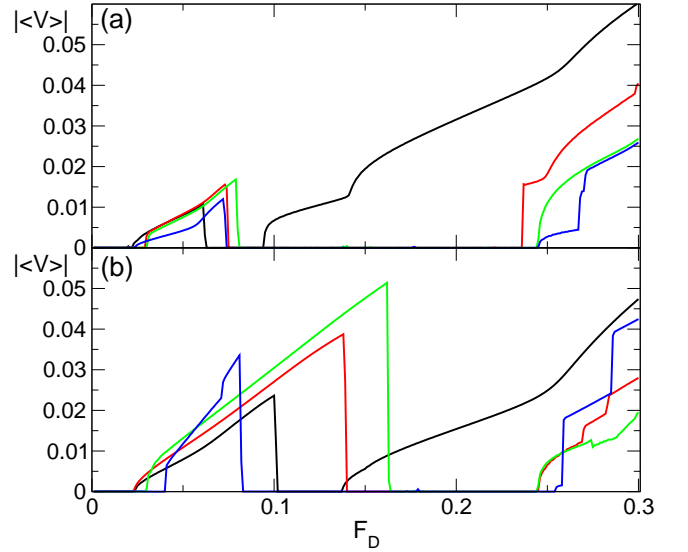


FIG. 7. (a) $|\langle V \rangle|$ vs F_D for driving in the hard direction at $N_c = 3.25$ (black), 4.25 (red), 4.75 (green), and 5.25 (blue). Each curve contains a reentrant pinning phase. (b) $|\langle V \rangle|$ vs F_D for $N_c = 5.5$ (black), 5.75 (red), 6.0 (green), and 8.0 (blue), also showing reentrant pinning.

plaquette varies from 2 to 5. Just above F_c , a rearrangement of the clogged state occurs into a partially clogged state where a small number of particles are able to push their way through the clog and begin to flow, as illustrated in Fig. 6(b) for $F_D = 0.2$. As the drive increases, the partially clogged configuration begins to break apart, as shown in Fig. 6(c) for $F_D = 0.26$ at the second jump in $|\langle V \rangle|$. Above this jump, the number of particles involved in the clog is reduced, as shown in Fig. 5(d) for $F_D = 0.3$. The size of the clog continues to decrease with further increases in F_D as additional particles join the flow, leading to additional steps in $|\langle V \rangle|$.

In Fig. 7(a) we plot $|\langle V \rangle|$ versus F_D for representative fillings of $N_c = 3.25, 4.25, 4.75$, and 5.25 , where in each case there is an interval of F_D over which reentrant pinning occurs. The clogging effects become stronger at the higher fillings, so that $F_{c2} \approx 0.25$. Figure 7(b) shows $|\langle V \rangle|$ versus F_D for $N_c = 5.5, 5.75, 6.0$, and 8.0 , which again exhibit reentrant pinning effects. The onset F_{rp} of the repinned state shows some variations but generally shifts to higher values of F_D for $N_c = 5.75$ and 6.0 .

In Fig. 8(a) we plot $|\langle V \rangle|$ versus F_D for $N_c = 8.25, 8.5, 8.75$, and 10.5 . Reentrant pinning occurs for $N_c = 8.25$ and $N_c = 8.75$, while at $N_c = 8.5$ and $N_c = 10.5$, there is only a single depinning transition but there is a transition from a pinned uniform state directly to a clogged inhomogeneous state. At higher values of N_c there are generally more steps and jumps in the sliding phases due to the increased number of particles participating in the partially clogged arrangements, which generates a larger number of partially clogged stages of flow.

In Fig. 8(b) we show $|\langle V \rangle|$ versus F_D for $N_c = 9.25$,

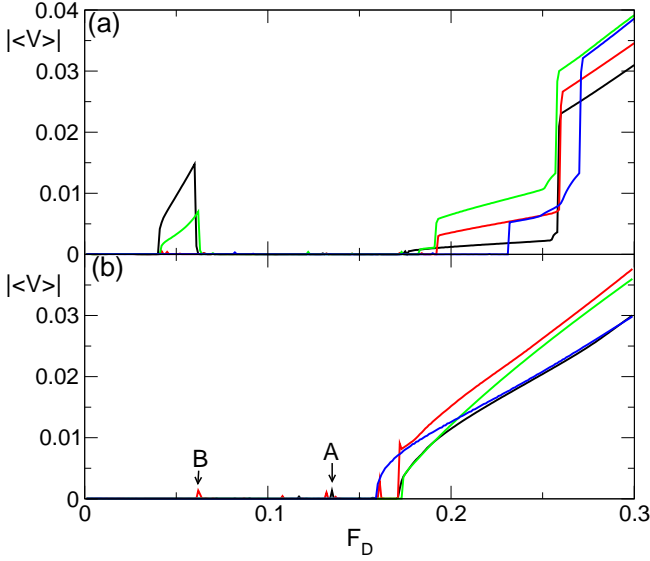


FIG. 8. $|\langle V \rangle|$ vs F_D for driving in the hard direction at $N_c = 8.25$ (black), 8.5 (red), 8.75 (green), and 10.5 (blue). There is a single depinning transition for $N_c = 8.5$ and $N_c = 10.5$, and at these fillings there is a direct transition from a pinned to a clogged state without an intermediate flowing state. (b) $|\langle V \rangle|$ vs F_D for $N_c = 9.25$ (black), 10.75 (red), 11.0 (green), and 12.0 (blue). The point marked A indicates the value of F_D at which there is a transition from the pinned to the clogged state for the $N_c = 9.25$ system, and the point marked B indicates the same transition for the $N_c = 10.75$ system.

10.75, 11.75, and 12.0. Each of these fillings exhibits only a single depinning threshold, but the transition from the uniform pinned state to the inhomogeneous clogged state can still be detected in the form of small jumps in $|\langle V \rangle|$ in the $N_c = 9.25$ and $N_c = 10.75$ curves. These jumps, marked by the letters A and B, are generated by a transient rearrangement of the particles in the pinned phase to produce a clogged structure. For $N_c \geq 11$ the system transitions directly from a pinned state to a flowing state without any kind of clogging. The particle density remains uniform and there are no jumps in $|\langle V \rangle|$, as shown in the $N_c = 11.0$ and $N_c = 12.0$ curves.

In Fig. 9 we plot a dynamic phase diagram as a function of F_D versus N_c created from a series of simulations that highlights the pinned phase, sliding phase, clogged phase, and reentrant sliding phase. In the pinned state, $|\langle V \rangle| = 0$ and the particles are distributed evenly throughout the system. In general, the depinning force F_c marking the end of the pinned phase shifts to higher F_D with increasing N_c . In the sliding states $|\langle V \rangle| > 0$, while the clogged state has $|\langle V \rangle| = 0$ with a heterogeneous distribution of particles in the funnel array. It is possible to identify additional dynamic regimes within the sliding state. For example, the moving particles are evenly spaced in the sliding states at low drives below F_{rp} , while in the sliding states for $F_D > F_{c2}$ the spacing between the moving particles is initially heterogeneous,

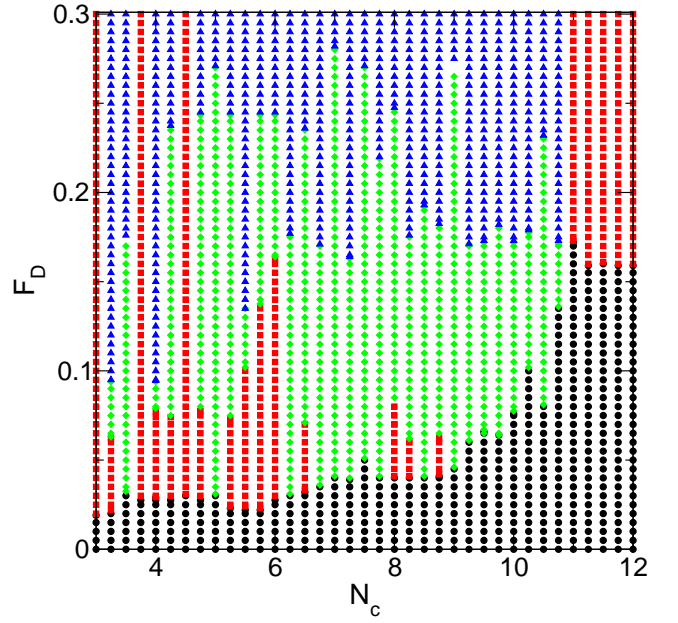


FIG. 9. Dynamic phase diagram as a function of F_D vs N_c . In the pinned phase (black circles), $|\langle V \rangle| = 0$ and the particle density is uniform. In the sliding phases, $|\langle V \rangle| > 0$. Red squares indicate the initial sliding phase and blue triangles indicate a reentrant sliding phase. In the clogged or reentrant pinned phase (green diamonds), $|\langle V \rangle| = 0$ and the particle density is heterogeneous.

but gradually become more homogeneous with increasing F_D as the clogs break apart. For $N_c > 6$, the pinned state can transition directly into a clogged state with no intermediate flowing phase, while for $N_c \geq 11$, the system passes directly from a uniform pinned state to a uniform moving state and the clogging behavior is lost. At low fillings $2.0 < N_c < 3.25$, there is only a pinned phase and a flowing phase, while for $3.25 < N_c < 11.0$ there are extended regions where clogging occurs. We note that due to the stochastic nature of the clogging, the value of F_D at which clogging first appears can vary from realization to realization when the filling is high enough for multiple particles to accumulate in a small number of plaquettes.

One question is how robust the clogged states are to the introduction of a finite temperature, which could break apart the clogged structures. To address this we measure the velocity-force curves at a finite temperature of $F^T = 0.1$, as shown in Fig. 10 for $N_c = 4.75$. At zero temperature, this filling exhibits an extended clogged region. Although the depinning transition at F_{c1} is unaffected by the addition of temperature, the onset of the clogged state shifts to higher F_D and the reentrant depinning transition F_{c2} shifts to lower F_D , giving a narrower clogged region. Thermal fluctuations produce numerous jumps in $|\langle V \rangle|$ as well as spikes of temporary flow within the clogged region due to the thermally assisted disintegration of clogged structures. Within the reentrant pinned region, the clogs rapidly reform, but in

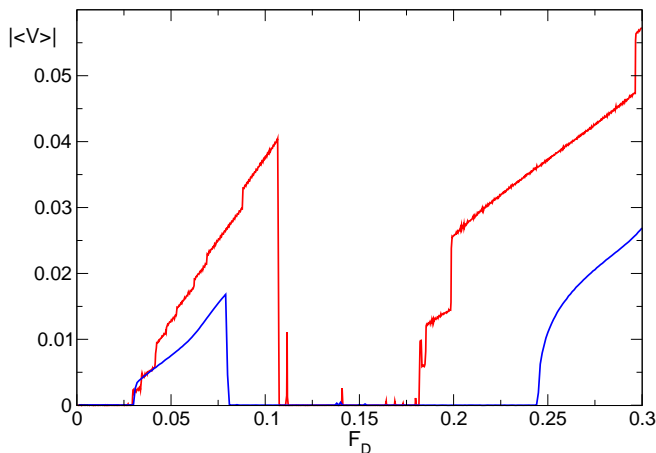


FIG. 10. $|\langle V \rangle|$ vs F_D at $N_c = 4.75$ for driving in the hard direction at zero temperature (blue) and at a finite temperature of $F^T = 0.1$ (red). At this filling there is an extended reentrant pinned region for $F^T = 0$. At finite temperature, the clogged region persists but is narrower, and it also contains a series of spikes in $|\langle V \rangle|$ that are produced by the thermal disintegration of a clog which then rapidly reforms.

the flowing regimes, the clogs are permanently destroyed and the net transport through the system is larger than at zero temperature. In general we find that in the range of F_D where the clogging susceptibility is high, clogging behavior still occurs for finite temperature but the clogging is interspersed with jumps or avalanche events, leading to a finite long-time average value of $|\langle V \rangle|$ which remains much lower than the average velocity in the flowing states.

We next discuss how the clogging we consider could be observed experimentally. One candidate realization is superconducting vortices in nanostructured asymmetric funnel arrays²⁵. A possible issue with this system is that the vortices are not true point particles, so that in the clogged state the vortices could merge and form multi-quantum flux configurations, causing the particle picture to break down. Such a state could still exhibit clogging, and there is the interesting possibility of studying a transition from a multi-quantum clogged vortex configuration to a flowing state, where the multi-quantum vortices would dissociate back into individual moving flux quanta. Random point pinning would likely add a stochastic element to the behavior of the superconducting vortices; however, there should still be extended regions of clogging dynamics at intermediate fillings. For systems such as magnetic skyrmions or bubbles, there is a similar issue in which the particle model can break down due to strong spatial distortions of the skyrmion or bubble. Such distortions could act to prevent clogging from occurring. Systems such as charged colloids or classical Wigner or ion crystals are also good candidates for observing the effects we describe. In granular or hard particle systems, reentrant clogging could occur; however, due to the strong contact interactions the system may remain

in a reentrant pinned or clogged state even for very high values of F_D , so that it could be difficult to observe the reentrant flowing state above F_{c2} .

Summary – In summary, we have investigated a system of repulsively interacting particles driven in the hard direction of an asymmetric funnel array for varied ratios of the number of particles to the number of funnel plaquettes. Previous work on this model focused on driving in the easy flow direction and showed only a single depinning threshold. In contrast, for driving in the hard direction we find that the system can exhibit a rich variety of dynamical phases including a reentrant pinned phase, where the system flows at lower drives but becomes pinned when the drive is increased. This reentrant pinning is the result of a clogging instability in which a buildup of particles in a small number of plaquettes block the flow of other particles. At higher drives, particles can force their way through the clog, leading to a second depinning transition. The clogging is a robust effect that occurs over the range of three to nearly eleven particles per plaquette. In addition to the reentrant pinning, we find that in some cases a partial clogging can produce negative differential conductivity, and we observe step-like features in the velocity-force curves due to the sequential breakup of a clog. We map the dynamic phases as a function of drive and filling fraction and identify a pinned phase where the particles are uniformly dense and do not move, a clogged phase where the particles do not move but are heterogeneously distributed with an accumulation of particles in certain plaquettes, and a moving phase. When a finite temperature is introduced, the clogging regime remains robust but exhibits intermittent bursts of flow when the clogs disintegrate under thermal fluctuations but then rapidly reform. Finally, we describe systems in which this clogging behavior could be observed, including superconducting vortices, colloids, Wigner crystals, or skyrmions in asymmetric channels.

This work was carried out under the auspices of the NNSA of the U.S. DoE at LANL under Contract No. DE-AC52-06NA25396.

- ¹Reichhardt C and Olson C J 2017 Depinning and nonequilibrium dynamic phases of particle assemblies driven over random and ordered substrates: a review *Rep. Prog. Phys.* **80** 026501
- ²Bhattacharya S and Higgins M J 1993 Dynamics of a disordered flux line lattice *Phys. Rev. Lett.* **70** 2617
- ³Blatter G, Feigel'man M V, Geshkenbein V B, Larkin A I and Vinokur V M 1994 Vortices in high-temperature superconductors *Rev. Mod. Phys.* **66** 1125
- ⁴Olson C J, Reichhardt C and Nori F 1998 Nonequilibrium dynamic phase diagram for vortex lattices *Phys. Rev. Lett.* **81** 3757
- ⁵Gruber G 1988 The dynamics of charge-density waves *Rev. Mod. Phys.* **60** 1129
- ⁶Williams F I B, Wright P A, Clark R G, Andrei E Y, Deville G, Glatli D C, Probst O, Etienne B, Dorin C, Foxon C T and Harris J J 1991 Conduction threshold and pinning frequency of magnetically induced Wigner solid *Phys. Rev. Lett.* **66** 3285
- ⁷Reichhardt C, Olson C J, Grønbech-Jensen N and Nori F 2001 Moving Wigner glasses and smectics: Dynamics of disordered Wigner crystals *Phys. Rev. Lett.* **86** 4354
- ⁸Pertsinidis A and Ling X S 2008 Statics and dynamics of 2D

- colloidal crystals in a random pinning potential *Phys. Rev. Lett.* **100** 028303
- ⁹Tierno P 2012 Depinning and collective dynamics of magnetically driven colloidal monolayers *Phys. Rev. Lett.* **109** 198304
- ¹⁰Bohlein T, Mikhael J and Bechinger C 2012 Observation of kinks and antikinks in colloidal monolayers driven across ordered surfaces *Nat. Mater.* **11** 126
- ¹¹Nagaosa N and Tokura Y 2013 Topological properties and dynamics of magnetic skyrmions *Nat. Nanotechnol.* **8** 899
- ¹²Reichhardt C, Ray D and Reichhardt C J O 2015 Collective transport properties of driven skyrmions with random disorder *Phys. Rev. Lett.* **114** 217202
- ¹³Barma M and Dhar D 1983 Directed diffusion in a percolation network *J. Phys. C: Sol. St. Phys.* **16** 1451
- ¹⁴Reichhardt C, Olson C J and Nori F 1998 Nonequilibrium dynamic phases and plastic flow of driven vortex lattices in superconductors with periodic arrays of pinning sites *Phys. Rev. B* **58** 6534
- ¹⁵Bénichou O, Illien P, Oshanin G, Sarracino A and Voituriez R 2014 Microscopic theory for negative differential mobility in crowded environments *Phys. Rev. Lett.* **113** 268002
- ¹⁶Reichhardt C and Reichhardt C J O 2018 Negative differential mobility and trapping in active matter systems *J. Phys.: Condens. Matter* **30** 015404
- ¹⁷Cecchi G A and Magnasco M O 1996 Negative resistance and rectification in Brownian transport *Phys. Rev. Lett.* **76** 1968
- ¹⁸Eichhorn R, Regtmeier J, Anselmetti D and Reimann P 2010 Negative mobility and sorting of colloidal particles *Soft Matter* **6** 1858
- ¹⁹Besseling R, Kes P H, Dröse T and Vinokur V M 2005 Depinning and dynamics of vortices confined in mesoscopic flow channels *New J. Phys.* **7** 71
- ²⁰Köppl M, Henseler P, Erbe A, Nielaba P and Leiderer P 2006 Layer reduction in driven 2D-colloidal systems through microchannels *Phys. Rev. Lett.* **97** 208302
- ²¹Barrozo P, Moreira A, Aguiar J and Andrade J 2009 Model of overdamped motion of interacting magnetic vortices through narrow superconducting channels *Phys. Rev. B* **80** 104513
- ²²Wilms D, Deutschländer S, Siems U, Franzrahe K, Henseler P, Keim P, Schwierz N, Virnau P, Binder K, Maret G and Nielaba P 2012 Effects of confinement and external fields on structure and transport in colloidal dispersions in reduced dimensionality *J. Phys.: Condens. Matter* **24** 464119
- ²³Dobrovolskiy O V, Begun E, Huth M and Shklovskij V A 2012 Electrical transport and pinning properties of Nb thin films patterned with focused ion beam-milled washboard nanostructures *New J. Phys.* **14** 113027
- ²⁴Piacente G and Peeters F M Pinning and depinning of a classic quasi-one-dimensional Wigner crystal in the presence of a constriction *Phys. Rev. B* **72** 205208
- ²⁵Yu K, Hesselberth M B S, Kes P H and Plourde B L T 2010 Vortex dynamics in superconducting channels with periodic constrictions *Phys. Rev. B* **81** 184503
- ²⁶Rees D G, Totsuji H and Kono K 2012 Commensurability-dependent transport of a Wigner crystal in a nanoconstriction *Phys. Rev. Lett.* **108** 176801
- ²⁷Zimmermann U, Smalenburg F and Löwen H 2016 Flow of colloidal solids and fluids through constrictions: dynamical density functional theory versus simulation *J. Phys.: Condens. Matter* **28** 244019
- ²⁸Wambaugh J F, Reichhardt C, Olson C J, Marchesoni F and Nori F 1999 Superconducting fluxon pumps and lenses *Phys. Rev. Lett.* **83**, 5106
- ²⁹Yu K, Heitmann T W, Song C, DeFeo M P, Plourde B L T, Hesselberth M B S and Kes P H 2007 Asymmetric weak-pinning superconducting channels: Vortex ratchets *Phys. Rev. B* **76** 220507(R)
- ³⁰Reichhardt C J O and Reichhardt C 2010 Commensurability, jamming, and dynamics for vortices in funnel geometries *Phys. Rev. B* **81** 224516
- ³¹Vlasko-Vlasov V, Benseman T, Welp U and Kwok W K 2013 Jamming of superconducting vortices in a funnel structure *Supercond. Sci. Technol.* **26** 075023
- ³²Karapetrov G, Yefremenko V, Mihajlović G, Pearson J E, Iavarone M, Novosad V and Bader S D 2012 Evidence of vortex jamming in Abrikosov vortex flux flow regime *Phys. Rev. B* **86** 054524
- ³³Lin N S, Heitmann T W, Yu K, Plourde B L T and Misko V R 2011 Rectification of vortex motion in a circular ratchet channel *Phys. Rev. B* **84** 144511
- ³⁴Redner S and Datta S 2000 Clogging time of a filter *Phys. Rev. Lett.* **84** 6018
- ³⁵To K, Lai P-Y and Pak H K 2001 Jamming of granular flow in a two-dimensional hopper *Phys. Rev. Lett.* **86** 71
- ³⁶Chevoir F, Gaulard F and Roussel N 2007 Flow and jamming of granular mixtures through obstacles *Europhys. Lett.* **79** 14001
- ³⁷Thomas C C and Durian D J 2013 Geometry dependence of the clogging transition in tilted hoppers *Phys. Rev. E* **87** 052201
- ³⁸Zuriguel I, Parisi D R, Hidalgo R C, Lozano C, Janda A, Gago P A, Peralta J P, Ferrer L M, Pugnali L A, Clément E, Maza D, Pagonabarraga I and Garcimartín A 2014 Clogging transition of many-particle systems flowing through bottlenecks *Sci. Rep.* **4** 7324
- ³⁹Barré C and Talbot J 2015 Cascading blockages in channel bundles *Phys. Rev. E* **92** 052141
- ⁴⁰Barré C and Talbot J 2015 Stochastic model of channel blocking with an inhomogeneous flux of entering particles *EPL* **110** 20005
- ⁴¹Nguyen H T, Reichhardt C and Reichhardt C J O 2017 Clogging and jamming transitions in periodic obstacle arrays *Phys. Rev. E* **95** 030902(R)
- ⁴²Helbing D, Farkas I J and Vicsek T 2000 Simulating dynamical features of escape panic *Nature (London)* **407** 487
- ⁴³Garcimartín A, Pastor J M, Ferrer L M, Ramos J J, Martín-Gómez C and Zuriguel I 2015 Flow and clogging of a sheep herd passing through a bottleneck *Phys. Rev. E* **91** 022808
- ⁴⁴Nicolas A, Bouzat S and Kuperman M N 2017 Pedestrian flows through a narrow doorway: Effect of individual behaviours on the global flow and microscopic dynamics *Trans. Res. B: Method.* **99** 30
- ⁴⁵Reichhardt C and Olson C J 2002 Colloidal dynamics on disordered substrates *Phys. Rev. Lett.* **89** 078301
- ⁴⁶Reichhardt C and Reichhardt C J O 2009 Random organization and plastic depinning *Phys. Rev. Lett.* **103** 168301
- ⁴⁷Liu A J and Nagel S R 2010 The jamming transition and the marginally jammed solid *Annu. Rev. Condens. Matter Phys.* **1** 347
- ⁴⁸Peter H, Libál A, Reichhardt C and Reichhardt C J O Crossover from jamming to clogging behaviors in heterogeneous environments arXiv:1712.03307